



# Why no anomaly is visible over most of the continent–ocean boundary in the global crustal magnetic field

Kumar Hemant\*, Stefan Maus<sup>1</sup>

*GeoForschungsZentrum, Telegrafenberg, 14473 Potsdam, Germany*

Received 18 February 2004; received in revised form 20 September 2004; accepted 29 October 2004

## Abstract

It is generally believed that an anomaly should be expected over the continent–ocean (C–O) boundary in the global magnetic anomaly maps. However, such maps prepared at satellite altitude do not show an anomaly over most of the C–O boundary. We address this issue by a forward modelling technique. We use a Geographic Information System (GIS) technique to integrate information of the various geological units of continents and oceans, the seismic crustal structure, and standard susceptibility values of the rock types and compute a global vertically integrated susceptibility (VIS) model. In addition, a remanent magnetisation model is used for the oceanic crust. Combining the induced and remanent magnetisation models, the crustal field anomaly is predicted at a satellite altitude of 400 km for spherical harmonic degrees 16–80. The results show that an anomaly is indeed not predicted over the C–O boundaries where the oceanic crust is flanked by continental regions Phanerozoic in age. We demonstrate that, largely, a C–O anomaly over these regions is not even expected in the global magnetic anomaly map for degrees 1–80, confirming that it is not a long-wavelength feature masked by the core field. An anomaly, however, is predicted over some parts of the C–O boundary where the flanking geological provinces over the continents are Precambrian in age. We argue that the VIS values for the continents and oceans are largely comparable and therefore no anomaly is expected over most of the C–O boundary.

© 2004 Elsevier B.V. All rights reserved.

*Keywords:* Continent–ocean anomaly; Global; Vertically integrated susceptibility (VIS)

## 1. Introduction

In the interpretation of global magnetic anomaly maps a startling question has been why no anomaly is observed over most parts of the C–O boundary (Meyer et al., 1983, 1985). Due to the difference in composition and thickness of continents and oceans, one would expect such an anomaly. Forward modelling methods based on global models of Meyer et

\* Corresponding author. Tel.: +49 331 2881271; fax: +49 331 2881235.

*E-mail address:* [hemant@gfz-potsdam.de](mailto:hemant@gfz-potsdam.de) (K. Hemant).

<sup>1</sup> Present addresses: CIRES, University of Colorado, Boulder, CO, USA; National Geophysical Data Center, National Oceanographic and Atmospheric Administration, Boulder, CO, USA.

al. (1983) and Hahn et al. (1984), derived from surface geology, seismic structure, and standard susceptibilities were used to study the effect of the vertically integrated magnetisation contrast between continents and oceans. The predicted magnetic field, in general, did not have an anomaly over the C–O boundary. It was therefore concluded that this effect might be a long wavelength feature, which has been removed with the long wavelength main field in producing the global crustal field anomaly maps. This inference was also supported by studies of Cohen (1989) and Council et al. (1991) who modelled the C–O boundary as a step function in susceptibility contrast. They confirmed that the C–O boundary is a long-wavelength feature and that it is partly removed in subtracting the long wavelength main field. Arkani-Hamed (1990), on the other hand, argued that the C–O boundary would be a small scale feature which is not seen in the satellite anomaly maps due to the lack of resolution. Hinze et al. (1991) compiled the mean magnetic anomaly amplitude for crustal anomalies and for oceanic anomalies off the coast of South America and found a statistical increase in continental anomaly amplitude. In another study, Hayling (1991) showed that the variation of Curie-isotherm in

the oceanic lithosphere matches well with the observed map prepared using Magsat satellite data. Following the work by Arkani-Hamed and Strangway (1986), he suggested that some of the anomalies observed in satellite anomaly maps over C–O boundaries along the coast of the Atlantic ocean are caused by thermal destruction of magnetic minerals in the upper oceanic mantle rather than by pronounced difference in vertically integrated magnetisation. Based on the Magsat derived magnetic anomaly map, Singh et al. (1991) defined the geological boundary of the continent and ocean across both the eastern and western coasts of the Indian peninsula. They concluded that there exists a sharp geological continent and ocean boundary on the east coast and a gradual transition in the west. SEMM models of Purucker et al. (1998), however, showed a signal over the C–O boundary which also affects the anomalies further inside the continents. Recently, Purucker et al. (2002) included the heat flow associated with the major tectonic provinces and studied the satellite anomaly observed over the Kentucky and Georgia region using a combined induced and remanent magnetisation model. The paper shows the complexity involved in detecting C–O boundary anomalies. The observed mag-

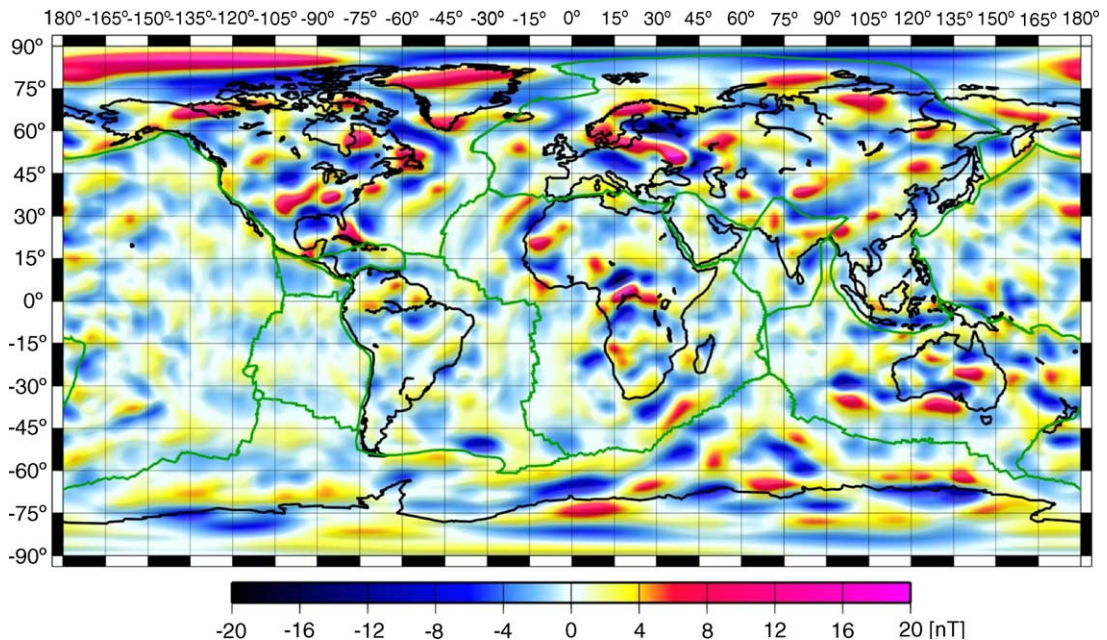


Fig. 1. Vertical component of the lithospheric magnetic field at 400 km altitude, as given by the MF2 model derived from CHAMP satellite magnetic measurements (<http://www.gfz-potsdam.de/pb2/pb23/SatMag/model.html>).

netic anomaly map shown in Fig. 1, is derived from the lithospheric field model MF2 (<http://www.gfz-potsdam.de/pb2/pb23/SatMag/model.html>) which is the first revision of an earlier model derived by Maus et al. (2002). This map, which can resolve anomaly features down to wavelengths of 500 km (degree 80), is used here to study the anomaly features over the continent–ocean boundary. The map shows an absence of anomalies over most of the C–O boundaries that are flanked by continental regions Phanerozoic in age. However, the regions over the southern coast of western Africa, over the coast of northwestern Africa, over the northern coast of Baltic Shield, over the northeast of Guyana Shield, South America, over the eastern coast of India and over the western coast of Australia primarily lie adjacent to Precambrian provinces are marked by prominent anomaly features. There are other interesting anomaly features observed over the Labrador Sea and over the regions parallel to the mid-oceanic ridges in the North Atlantic Ocean. There are additional strong anomaly features observed over the eastern coast of Indian subcontinent. In the present work, therefore, we seek to answer: (1) why an anomaly is not seen in the global magnetic anomaly maps over most of the C–O boundary and (2) whether the anomaly over the C–O boundary is a long wavelength feature and hence masked by the core field. These key questions were also raised in a recent comprehensive treatise on the Earth's magnetic field by Langel and Hinze (1998).

## 2. Forward modelling

### 2.1. Global vertically integrated susceptibility model

A global crustal magnetisation model is derived using a GIS based forward modelling technique. We use the map of world geology (CGMW, 2000) which shows the distribution of various geological provinces based on geological age but does not detail the rock types. The information of the rock types is supplemented from a compilation of various tectonic maps (Goodwin, 1991). Global seismic models 3SMAC (Nataf and Ricard, 1996) and CRUST2.0 (Bassin et al., 2000) are used as the thickness of the magnetised crust. This is based on our assumption that the Moho is a magnetic

boundary (Wasilewski and Mayhew, 1992). Thus, the upper mantle is considered to be non-magnetic. The last sources of information are the standard volume susceptibility values for various rock types compiled from standard sources (Clark and Emerson, 1991; Hunt et al., 1995).

To derive a global magnetisation model of the crust, all of the known rock types for a particular geological region are compiled and, using their maximum volume susceptibility value, an average susceptibility value is computed and assigned to this region. Next, using the global seismic crustal structure, a vertically integrated susceptibility (VIS) model is computed by taking the product of susceptibility and thickness at each point of the region. All Precambrian and Phanerozoic provinces of the world are assigned susceptibility values according to the modelling procedure described in Hemant and Maus (2004). To model the oceans, the oceanic crust is divided into three layers following White et al. (1992). Layer 1 (0.0 SI), 0–1 km thick, is sediment. Layer 2 (0.066 SI), the middle layer, is  $2.11 \pm 0.55$  km thick and is subdivided into an upper portion of extruded basalt, layer 2A, and a lower portion of basalt, massively intruded by dikes, layer 2B. Layer 3 (0.049 SI) is gabbroic, with an average thickness of about  $4.97 \pm 0.90$  km. The numbers in parentheses give the susceptibility values used for the rock types (Clark and Emerson, 1991; Hunt et al., 1995). The VIS values for the oceans are computed by multiplying the susceptibility values of the individual oceanic layers with their average thicknesses. The global VIS map is derived by knitting together the VIS values for the continents and oceanic regions (Hemant and Maus, 2004; Hemant, 2003 (<http://www.diss.fu-berlin.de/2003/270/indexe.html>)). Fig. 2 shows the global VIS model taken from Hemant and Maus (2004).

### 2.2. Bulk remanent magnetisation model

Within the continents, stable remanence is likely to be less important in deep crustal conditions than in upper crustal conditions (Shive et al., 1992). Treloar et al. (1986) showed through laboratory and theoretical studies that even viscous remanent magnetisation in the lower crust cannot be as great as induced magnetisation. Based on the size of Fe–Ti oxides in the lower crust, which are generally composed of multi-domained crystals, Shive (1989) and Shive et al. (1992)

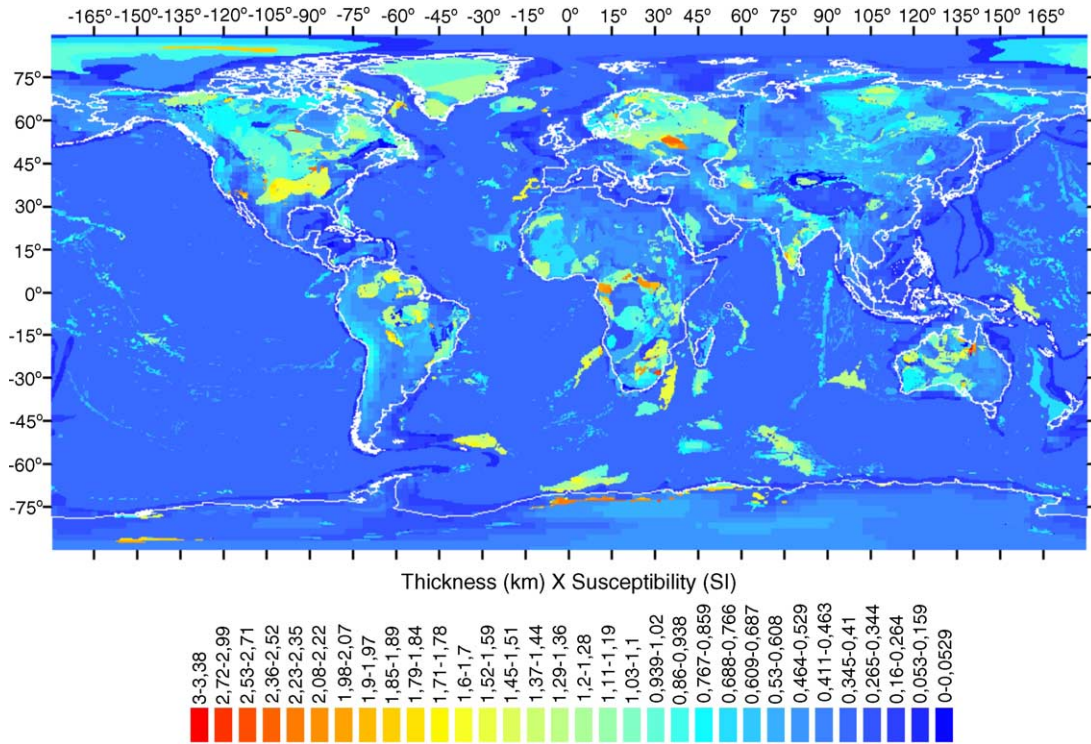


Fig. 2. Vertically integrated susceptibility (VIS) map of the world.

concluded that the total magnetisation of lower crustal rocks is not significantly greater than their induced magnetisation. However, studies of anomaly maps over East European Craton using Magsat data (Taylor and Ravat, 1995, 1997; Pucher and Wonik, 1997, 1998) find indications for remanence in the lower continental crust of Europe. They could not completely explain the observed anomalies just by induced magnetisation of the crust. This result is also confirmed by the recent analysis of CHAMP magnetic anomaly maps over Europe (Hemant and Maus, 2004). There is also evidence from the modelling results over western and central Africa (Hemant and Maus, 2004) that either the magnetised lower crust extends deeper, or magnetisation extends into the upper mantle, or significant remanent magnetisation of the lower crust is also contributing to the observed anomaly. Due to non-uniqueness, it is generally difficult to separate the individual contribution of induced and remanent magnetisation to the observed anomaly (Maus and Haak, 2003). Since the composition and remanent magnetisation content of the

lower crust is largely unknown, except for some regions where the lower crust is exposed (Fountain and Salisbury, 1981), it is difficult to confidently estimate its remanent magnetisation. An approach taken by Whaler and Purucker, (2003) in computing global models of the lithospheric magnetisation from satellite data, including both induced and remanent magnetisation, was to invert for the minimal magnetisation explaining the observed anomalies.

The continental deep drilling program in Germany (KTB) shows a dominance of pyrrhotite ferromagnetic minerals in metabasites and gneisses at shallow depths (<7800 m) while magnetite is dominant in marble- and calcisilicate-bearing amphibolites and meta-ultramafics from the depth range 7320–7800 m (Berckhemer et al., 1997). Unfortunately, most of the KTB rocks are carriers of unstable natural remanent magnetisation (NRM) (Pohl et al., 1991; Worm and Rolf, 1994), which are of chemical or thermochemical origin (Berckhemer et al., 1997). These remanences do not contribute significantly, compared with the induced magnetisation.

Moreover, remanent magnetisation content over most of the continents are largely unknown as indicated by Purucker et al. (2002), hence, remanence is not considered in the derivation of our crustal magnetisation model for the continents.

Over the oceans, the magnetic strips of alternate polarity parallel to the mid-oceanic ridges, so prominent in the aeromagnetic maps (Verhoef et al., 1996), are mostly absent at satellite altitude. This is because fields from the alternating remanent magnetisation of the spreading oceanic crust nearly cancel at satellite altitude (LaBrecque and Raymond, 1985). However, there are strong anomaly features parallel to the mid-oceanic ridges prominent over the North Atlantic Ocean and off the coast of the Indian peninsula (Fig. 1). These zones of remanent magnetisation have been associated with the Cretaceous Quiet Zones (KQZ), their magnetisation acquired during the Cretaceous Long Normal (CLN) polarity interval (LaBrecque and Raymond, 1985; Cohen and Achache, 1994; Purucker et al., 1998; Dyment and Arkani-Hamed, 1998; Purucker and Dyment, 2000). As these zones of remanent magnetisation contribute significant anomalies at satellite altitude, these zones of alternate magnetisation should be modelled. Remanent magnetisation of the oceanic crust arises due to a combination of primary and secondary magnetisation. The primary magnetisation is called thermo remanent magnetisation (TRM) while the secondary magnetisation is often attributed to chemical remanent magnetisation (CRM) (Butler, 1992). The magnetic anomaly pattern observed over the oceans is due to the intensity and the direction of the bulk remanent magnetisation of the oceanic floor formed in different geological age in last 200 years. The intensity of the bulk remanent magnetisation of the oceanic crust is the combined effect of primary and secondary magnetisation (Raymond and LaBrecque, 1987).

We compute the intensity and direction of the remanent magnetisation using the digital isochron map of the oceanic crust (Müller et al., 1997), the decay model of primary and secondary magnetisation, superimposed on the polarity of the isochrons (Gradstein et al., 1994; Cande and Kent, 1995) and following procedures outlined by Dyment and Arkani-Hamed (1998). The directions of the bulk remanent magnetisation for each oceanic age floor is computed using rotation models of Royer et al., (1992) combined with the apparent polar wander path for Africa following the work of

Dyment and Arkani-Hamed (1998). The crustal model for the oceanic region is same as used for derivation of VIS model. The intensity and remanent magnetisation vectors used in this paper are taken from Hemant and Maus (2004).

Our global crustal magnetisation model does not account for variations in Curie-temperature depth (CTD) within the crust. The reason is that accurate temperature information is not available for most areas of the world. Arguably the most accurate temperature model, by Artemieva and Mooney (2001), has a lateral resolution of only  $10^\circ \times 10^\circ$ , which again would not reveal much about the temperature variation within a region of small lateral extent like continental margins and subduction zones. Moreover, the absence of magnetites in mantle peridotites, except in few pockets of serpentinized upper mantle (Haggerty, 1978) led Wasilewski and Mayhew (1992) to conclude that the Moho is the lower magnetic boundary. Over the oceans, serpentinized upper mantle as argued by Arkani-Hamed and Strangway (1986) and Arkani-Hamed (1988), could add to anomalies observed at satellite altitude. However, their studies were restricted to subduction zones. Thus, the present global crustal magnetisation model does not include the temperature information relying on the more accurately known Moho as a lower magnetic boundary, instead.

The derived global VIS and bulk remanent magnetisation model, discussed in the above two sections, are used separately as the input to the equivalent dipole method to compute the magnetic potential at a height of 400 km above the mean Earth radius (Hemant and Maus, 2004). The potential is further expanded into spherical harmonics to derive the Gauss coefficients of the predicted field. The vertical field anomaly map is computed from these Gauss coefficients and spherical harmonic degrees 1–15 are set to zero in the initial interpretation because this long wavelength crustal field is masked by the main field and therefore is not observable. Later, for Fig. 5, we also display degrees 1–15.

### 3. Comparison of mean VIS contrast for continents and oceans

In the previous section, the global VIS model is derived by integrating susceptibility values for various geological provinces. Since the lateral variation of

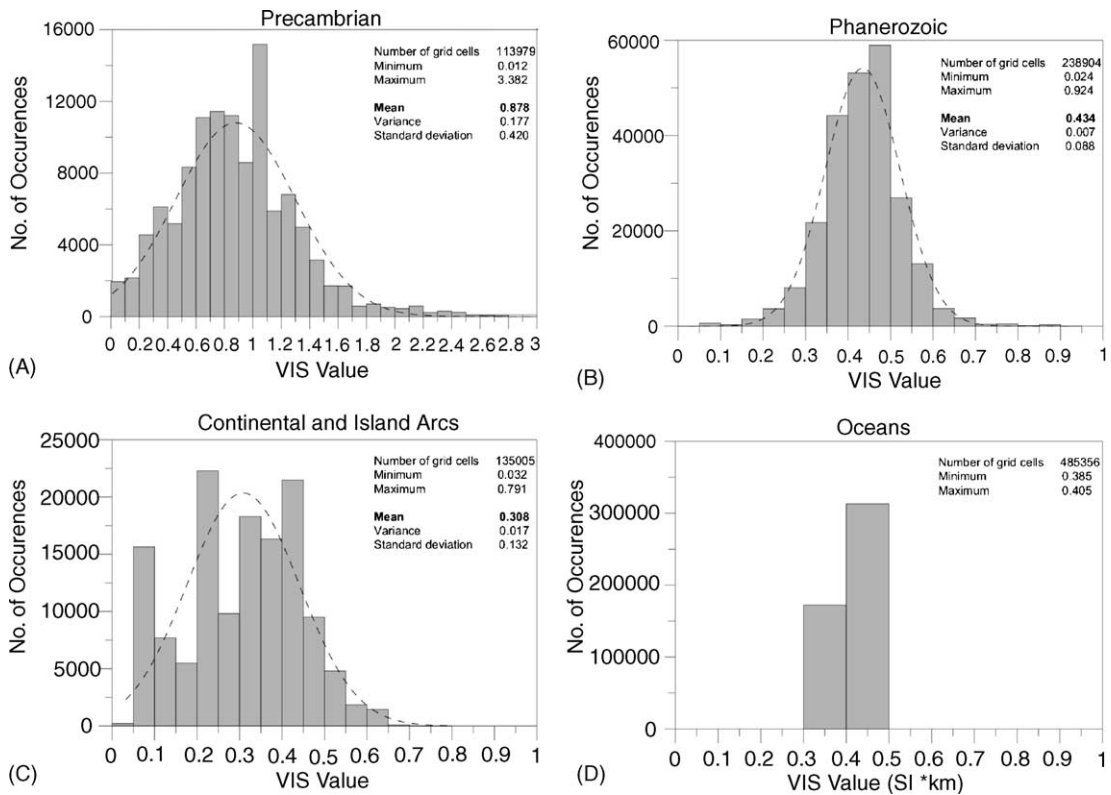


Fig. 3. Mean vertically integrated susceptibility (VIS) values shown for various geological provinces of the continents and oceans: (A) Precambrian provinces, includes Archeans and Proterozoics, (B) Phanerozoic provinces, (C) Continental and Island Arcs and (D) all major oceanic regions of the world. The curves (dashed lines) show the Gaussian fit to the data.

the VIS is responsible for the magnetic anomalies at satellite altitude, let us take a closer look at the distribution of these VIS values separately for the continental and oceanic regions. A statistical analysis of Magsat magnetic anomalies by Hinze et al. (1991) showed the combined magnetic anomaly power of the continents to be nearly 15% greater than that of the oceans. On this basis, they asserted that the magnetisation of the oceans is significantly greater than the continents considering a 6 km thick oceanic crust and 40 km thick continental crust. More subtle evidence for the VIS difference between continents and oceans can be obtained by statistically analysing the distribution of the VIS map displayed in Fig. 2. The resolution of the VIS model is  $0.25^\circ \times 0.25^\circ$ , which makes a total of 1,036,800 grid cells. These cells over the continents include the Archean, Proterozoic and Phanerozoic provinces. Continental and Island Arcs, oceanic crust and oceanic plateaus occupy the oceanic

regions. Histograms of these VIS distributions for various geological provinces, viz., Precambrian, Phanerozoic, Continental and Island Arcs and oceans are given in Fig. 3. The histogram in Fig. 3D for the oceans does not include the oceanic plateaus, as these bear no significance for this work. Each histogram shows the mean, standard deviation, and total number of grid cells, along with the maximum and minimum VIS value of the province. The histograms show a Gaussian distribution of the data points for the continental regions (Fig. 3A and B) and the curves (dashed lines) are Gaussian fit to the data. The histogram for the Continental and Island Arcs also follow a Gaussian distribution with a mean 0.308 SI km and standard deviation 0.132 SI km but peaks at 0.075 SI km and 0.225 SI km are also evident (Fig. 3C). The histogram for oceans shows only two peak values of 0.385 SI km and 0.405 SI km (Fig. 3D). This is because of our choice of crustal model, which includes two broad subdivisions of oceanic crust, based

on its geologic age. The crust having age  $<34$  Ma is classified as young crust while  $>34$  Ma is classified as old crust (White et al., 1992). Following White et al. (1992), the old crust is assumed thicker by 400 m from the young crust. The important parameter, however, for the oceanic region is the VIS value of the old crust (0.405 SI km) which engulfs most of the continents except the western coast of North and South American craton (CGMW, 2000), where the VIS value of the young oceanic crust (0.385 SI km) is more important.

The mean VIS values for continental regions are, in general, greater than the oceans. The mean VIS value for Precambrian provinces is 0.878 SI km with a standard deviation of 0.42 SI km (Fig. 3A). This is nearly twice the mean VIS value (0.434 SI km) for Phanerozoic provinces with a standard deviation of 0.088 SI km (Fig. 3B). This maximum VIS value of the oceans is nearly two times smaller than the mean VIS value for the Precambrian provinces while it is comparable with the mean VIS values for the Phanerozoic provinces. These differences in VIS values in turn should have a direct influence on the amplitude of the magnetic anomalies expected over the continental and oceanic regions. Thus, it is expected to have a higher magnetic anomaly contrast at satellite altitude over the C–O regions, where the oceanic regions are flanked by geological provinces Precambrian in age, while almost negligible contrast over regions flanking Phanerozoic provinces. The VIS values over the continental and Island Arcs are less significant where the horizontal dimension of the Arcs is less than 500 km, this being the resolution of the observed CHAMP magnetic anomaly map, but could be comparatively significant in regions where the width is more than 500 km, such as in continental margins of Bering Sea, south of Kamchatka peninsula, Russia, South China Sea, eastern region of Newfoundland, North America and almost all of the northern margins of Europe and Russia (CGMW, 2000). Some continental margins flanking the Indonesian islands may also be significant.

#### 4. Preliminary results

The predicted anomaly map for the vertical component of the magnetic field for degrees 16–80, derived from the global crustal magnetisation model discussed in Section 2, is shown in Fig. 4. The figure shows strong

anomaly features over the continents while moderate to weak anomaly features over the oceans. The anomalies predicted over the Cretaceous Quiet Zones are reproduced well, especially over the North and the South Atlantic Ocean (Hemant and Maus, 2004). The anomalies over the Precambrian provinces of the continents dominate over the anomalies over the younger Phanerozoic crust, which are rather weak in amplitude. Furthermore, the major anomaly features over the Precambrian provinces in the predicted map are in agreement with the observed magnetic anomaly map. Anomalies over the C–O boundary are largely absent, as can be seen for the continental regions of central-east Africa, the west coast of South America and even most of the south-east South American continent, western coast of North America and the entire eastern coast of Asia and Russia and parts of eastern Australia. These regions are occupied by younger continental rock types Phanerozoic in age.

There are, however, anomaly features predicted over the coast of northwest Africa (1.10–1.60 SI km), over the north of the Baltic Shield (0.67–1.60 SI km), over the northeast of Guyana Shield (1.39–1.60 SI km) and off the western coast of Australia (0.77–1.56 SI km). The numerical values shown in parenthesis show the variation of VIS value associated with these geological regions. These regions are Precambrian in age and, an anomaly is predicted over the adjacent C–O boundary, due to their high VIS contrast compared with that of the oceans (0.38–0.40 SI km). The predicted anomaly patterns are largely in agreement with the observations. These results are also in agreement with the predictions from the histograms showing the distribution of mean VIS values for Precambrian and Phanerozoic provinces with respect to the VIS value for the oceans (Fig. 3).

It is important to emphasize here that the observed anomaly map is partly contaminated by short wavelengths (spherical harmonic degrees 16–20) from the core (Arkani-Hamed and Strangway, 1985; Harrison et al., 1986), which are prominently seen over the Pacific Ocean as alternate stripes of positive and negative anomaly (Fig. 1). Such contaminations also hamper interpreting the signals whose sources lie only in the crust. The predicted anomaly map is free of such contaminations and thus helps to distinguish anomaly features over the C–O boundary. There are also anomaly features over the oceans, flanked by Phanerozoic con-



Fig. 4. Predicted vertical field anomaly map for degrees 16–80 at an altitude of 400 km.

tinental regions, which are due to either, subduction zones, viz., Aleutian arc (Clark et al., 1985) in the northern Pacific region, and southwest coast of Mexico (Council and Achache, 1987) or with oceanic plateaus, especially off the eastern coast of Australia and southern coast of Africa. The strong negative anomaly features over the Labrador Sea, situated between Greenland and the North American craton, could be a result of higher VIS value on both sides of the continents as compared to the smaller value of the Labrador Sea (Bradley and Frey, 1991). But in general, anomalies over most of the C–O boundary are absent in the predicted anomaly map.

##### 5. Is the C–O boundary a long wavelength feature?

As it is now evident from the preliminary investigation that most of the C–O boundary is not expected to be visible in the magnetic anomaly map for wavelengths corresponding to degrees 16–80, can this then lead to an inference that the C–O boundary is a long wavelength feature and that it was removed while removing the lower harmonic degrees 1–15, as has been asserted

by Meyer et al. (1983) and Cohen (1989)? This question can be answered by computing an anomaly map comprising all the harmonics. This means to predict the lithospheric field for degrees 1–15, which are not observable since they are masked by the main field. As the predicted anomaly map (Fig. 4) was computed for degrees 16–80 using the global VIS model, the same model can also be used to predict the long wavelength components of the crust. Following the same procedure as stated in Section 2, the vertical field magnetic anomaly map for degrees 1–80 is predicted at a satellite altitude of 400 km. The anomaly map (Fig. 5) shows the presence of strong anomaly features at the edges of the major cratons of the world. Interestingly, there are some additional weak anomaly features all over the western coast of the North American craton and central African region. As compared to predicted anomaly map for degrees (16–80), the anomaly features over the C–O boundaries adjacent to geological provinces Precambrian in age, becomes stronger in amplitude, but only a marginal change is noticed over the C–O boundaries adjacent to younger Phanerozoic provinces. Largely, however, an anomaly over most of the C–O boundary is not evident in the map. Thus, we conclude that the possible C–O boundary anomaly is not a

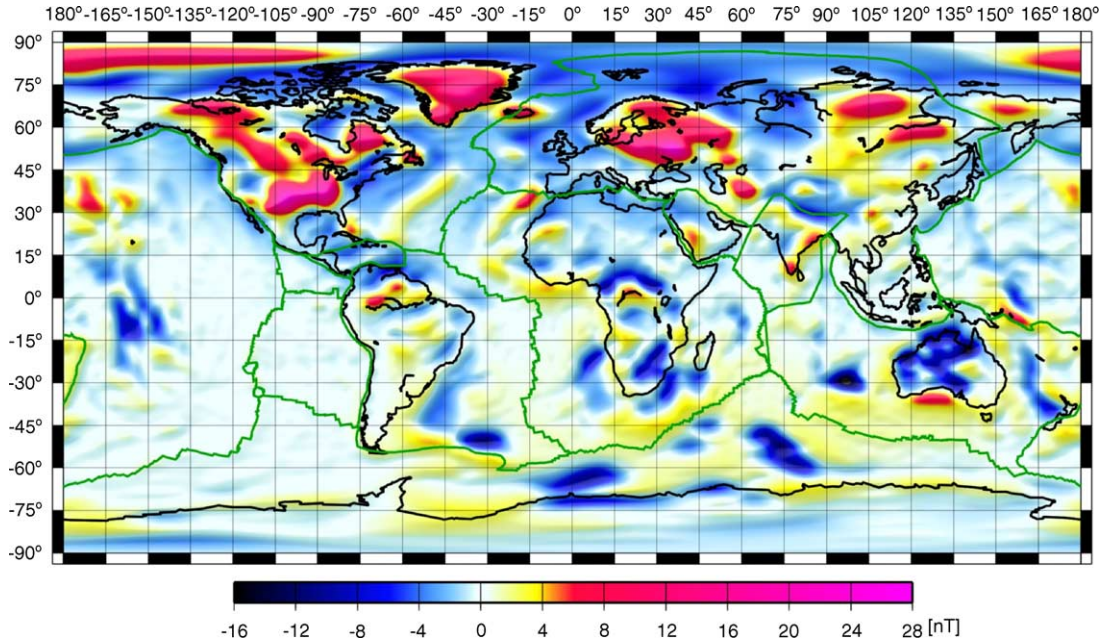


Fig. 5. Predicted vertical field anomaly map for degrees 1–80 at an altitude of 400 km.

long wavelength feature which is masked by the core field.

**6. Can the C–O boundary be visible at all at satellite altitude?**

However, as the C–O boundary gets clearly demarcated in aeromagnetic compilations (see for instance Verhoef et al., 1996) then is it that these anomalies are attenuated so much that they are not observed at satellite altitude? Let us investigate the conditions under which this anomaly would be visible. This problem is studied by deriving new global VIS models that have an unrealistically high or low susceptibility value for oceans. With this approach we study whether a stronger susceptibility contrast would generate a visible C–O anomaly at satellite altitude.

Two extreme values of susceptibility for oceanic regions are considered. Case-0 assumes a susceptibility value of zero, while Case-2 takes two times the susceptibility value already used in deriving the VIS model displayed in Fig. 2. The susceptibility distribution is shown in Table 1. The VIS model is computed using the same procedure as described in Section 2. The ver-

tical field anomaly maps for degrees 16–80 are computed for these two VIS models along with the same remanent magnetisation model as input. As the global anomaly map shows several anomaly features, the results are shown, along with the observed and predicted vertical field anomaly maps, only for the North American craton in Fig. 6.

The observed vertical field anomaly map over the North American craton is shown in Fig. 6A. The anomaly features in the Pacific Ocean west of the craton are short wavelength contributions (degrees 16–20) from the core field (Arkani-Hamed and Strangway, 1985; Harrison et al., 1986). The anomalies over the eastern coast and over the Labrador Sea, situated between Greenland and the North American craton, is already explained in Section 1. However, the anomaly over the C–O boundary is not observed. Fig. 6B shows a

Table 1

The susceptibility distribution of continents and oceans which were used to study the C–O boundary effect

Geological region	Predicted	Case-0	Case-2
Continents	Orig. VIS	Orig. VIS	Orig. VIS
Oceans	Orig. VIS	0.0	2 × Orig. VIS

Orig. in columns (2–4) stands for the predicted VIS value in Fig. 2.

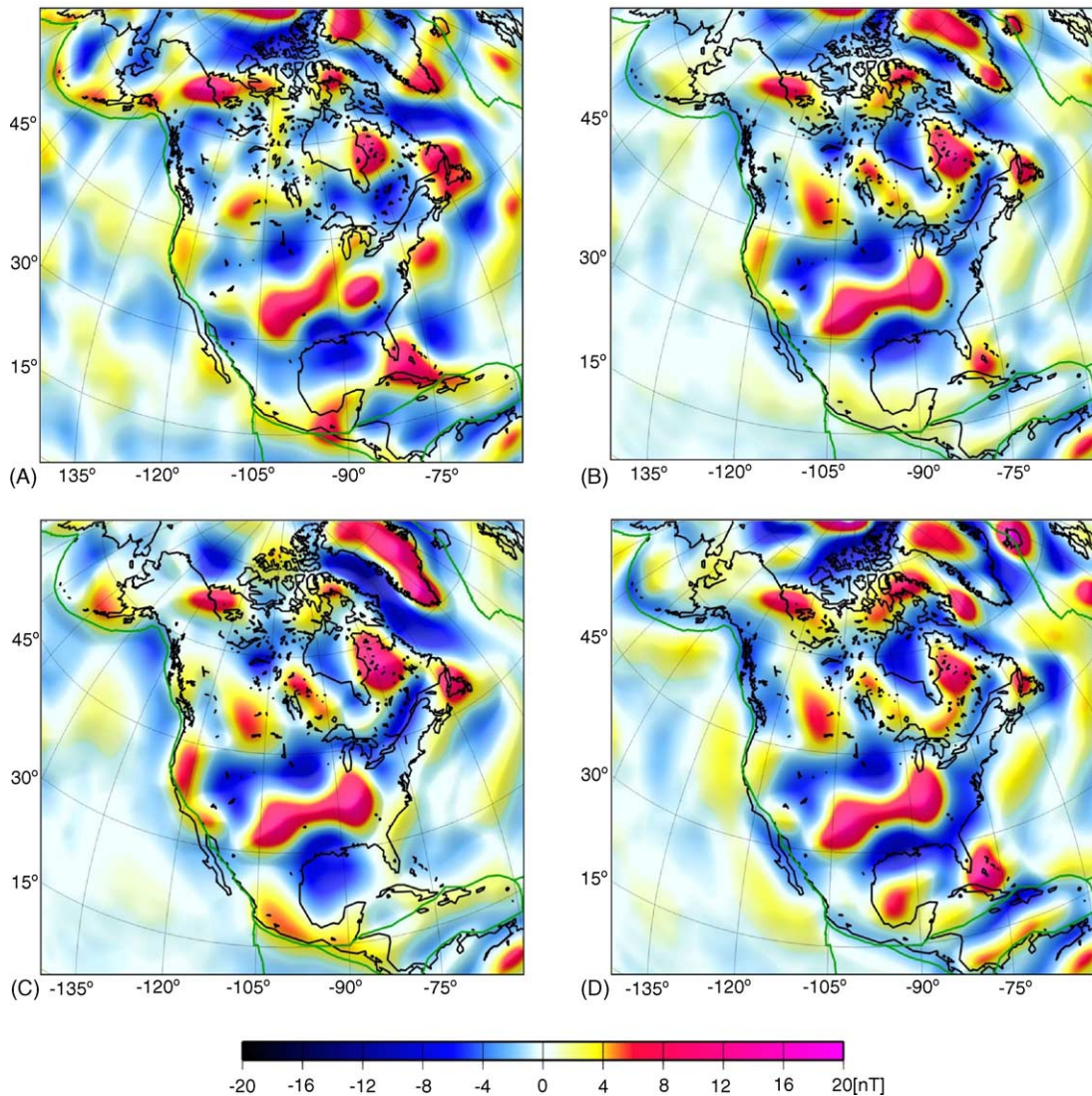


Fig. 6. Vertical field anomaly map for degrees 16–80 for (A) observed, (B) predicted, (C) Case-0 and (D) Case-2, at an altitude of 400 km.

few weak anomalies along the southern coast of Alaska and over the Labrador Sea, but an anomaly over the C–O boundary is not evident as well. The anomaly map derived using Case-0 is shown in Fig. 6C. All along the eastern coast of the North American craton, a negative anomaly feature is seen, which is more intense over the Labrador Sea. A positive anomaly is seen over some regions of the eastern coast. Anomalies over the western coast of Mexico and USA also appear stronger. The vertical field anomaly map pre-

dicted using Case-2 is shown in Fig. 6D. An evident positive anomaly is seen along the western C–O boundary of the North American craton, which extends from Alaska to Mexico. Similar signatures are also noticed over the central region of the eastern coast. The intense negative anomaly seen over the Labrador Sea in Fig. 6A and C now shows a positive anomaly over the northern region of the sea. Anomalies over the western and eastern continental region of USA are also modified now. Strong positive anomalies over the

Gulf of Mexico and banks of Florida are also seen in the map, which were partly or completely missing in Fig. 6C.

The above comparative study shows the sensitivity of satellite magnetic anomaly to the C–O boundary anomalies. Especially over the coastal regions of USA and Mexico the above result demonstrates that with a strong VIS contrast between continents and oceans, an anomaly over the C–O boundary would be seen at satellite altitude. The absence of such anomalies in the observed anomaly map (Fig. 6A) is therefore a significant result.

## 7. Conclusions

The predicted vertical field anomaly map for spherical harmonic degrees 1–80 comprising the long wavelength component of the crust (Fig. 5) shows largely no anomaly signatures over most of the C–O boundary. Therefore, the C–O boundary is not a long wavelength feature. This result is in contradiction to earlier investigations claiming that the C–O boundary is a long wavelength features (Cohen, 1989; Counil et al., 1991; Purucker et al., 1998). Anomalies over most of the C–O boundary, especially flanked by geological provinces of Phanerozoic in age, are also neither predicted nor observed in the visible magnetic anomaly field of degrees 16–80. There are, however, anomaly features – both observed and predicted – over the C–O boundary along Precambrian provinces. This suggests that the absence of an anomaly over most of the C–O boundary is due to the comparable VIS of the younger continental regions and oceans. This is also suggested from the comparable VIS values for the Phanerozoics and oceans (see Figs. 2 and 3) which are smaller than the VIS values for the Precambrian provinces. The results indicate that no C–O anomalies predicted over most of the C–O boundaries is just an indication that these anomalies do not exist at long wavelength. It is also possible that within the Phanerozoic provinces of the world significant contrast of susceptibility value could exist and such a contrast could produce an anomaly over the C–O boundary. Such a variation in susceptibility contrast within Phanerozoic provinces is not modelled and discussed in the present global VIS map. The predicted results from Case-0 and Case-2 show that significant VIS contrasts between oceanic and continental crust

would produce visible anomalies. This indicates that a significant VIS contrast between the continents and oceans, as between the Precambrian provinces and the oceans (Fig. 3) would produce a visible anomaly at the satellite altitude.

While a C–O boundary anomaly is largely absent in the observed map for degrees less than 80, small wavelength C–O anomalies can be expected for degrees beyond 80. Indeed, small-scale anomalies are visible in aeromagnetic anomaly maps, generally prepared at an altitude of less than 5 km. Thus, future higher resolution global magnetic anomaly maps may be helpful in resolving not only small wavelength features on the continents but would also further constrain the bulk susceptibility contrast between oceanic and continental lithosphere.

## Acknowledgements

We thank Michael Purucker, Patrick Taylor and an anonymous reviewer for providing constructive comments on this manuscript. Figs. 1 and 4–6 are prepared using GMT.

## References

- Arkani-Hamed, J., 1988. Remanent magnetization of the oceanic upper mantle. *Geophys. Res. Lett.* 15, 48–51.
- Arkani-Hamed, J., 1990. Magnetization of the oceanic crust between the Labrador Sea. *J. Geophys. Res.* 95, 7101–7110.
- Arkani-Hamed, J., Strangway, D.W., 1985. Lateral variations of apparent magnetic susceptibility of lithosphere deduced from Magsat data. *J. Geophys. Res.* 90, 2655–2664.
- Arkani-Hamed, J., Strangway, D.W., 1986. Effective magnetic susceptibility anomalies of the oceanic upper mantle derived from Magsat data. *Geophys. Res. Lett.* 13, 999–1002.
- Artemieva, I.M., Mooney, W.D., 2001. Thermal thickness and evolution of Precambrian lithosphere: a global study. *J. Geophys. Res.* 106, 16387–16414.
- Bassin, C., Laske, G., Masters, G., 2000. The current limits of resolution for surface wave tomography in North America. *EOS Trans. AGU* 81, F897.
- Berckhemer, H., Rauen, A., Winter, H., Kern, H., Kontny, A., Lienert, M., Nover, G., Pohl, J., Popp, T., Schult, A., Zinke, J., Soffel, H.C., 1997. Petrophysical properties of the 9-km deep crustal section at KTB. *J. Geophys. Res.* 102, 18337–18363.
- Bradley, L.M., Frey, H., 1991. Magsat magnetic anomaly contrast across Labrador sea passive margins. *J. Geophys. Res.* 96, 16161–16168.

- Butler, R.F., 1992. Paleomagnetism: Magnetic Domains to Geologic Terranes. Blackwell Scientific Publications (<http://www.geo.arizona.edu/Paleomag/book/>).
- Cande, S.C., Kent, D.V., 1995. Revised calibration of the geomagnetic polarity timescale for the Late Cretaceous and Cenozoic. *J. Geophys. Res.* 100, 6093–6096.
- Clark, S.C., Frey, H., Thomas, H.H., 1985. Satellite magnetic anomalies over subduction zones: the Aleutian arc anomaly. *Geophys. Res. Lett.* 12, 41–44.
- Clark, D.A., Emerson, D.W., 1991. Notes on rock magnetization characteristics in applied geophysical studies. *Expl. Geophys.* 22, 547–555.
- Cohen, Y., 1989. Traitements et interpretations de données spatiales en géomagnétisme: étude des variations laterales d'aimantation de la lithosphère terrestre. Ph.D. Thesis. University of Paris VII and Institute de Physique du globe de Paris.
- Cohen, Y., Achache, J., 1994. Contribution of induced and remanent magnetization to long-wavelength oceanic magnetic anomalies. *J. Geophys. Res.* 99, 2943–2954.
- Counil, J.-L., Achache, J., 1987. Magnetization gap associated with tearing in the central America subduction zone. *Geophys. Res. Lett.* 14, 1115–1118.
- Counil, J., Cohen, Y., Achache, J., 1991. A global C–O magnetization contrast: spherical harmonic analysis. *Earth Planet. Sci. Lett.* 103, 354–364.
- CGMW, 2000. Geological map of the world. Commission for the Geological Map of the World (CGMW)®. UNESCO Publishing.
- Dyment, J., Arkani-Hamed, J., 1998. Contribution of lithospheric remanent magnetization to satellite magnetic anomalies over the world's oceans. *J. Geophys. Res.* 103, 15423–15441.
- Fountain, D.M., Salisbury, M.H., 1981. Exposed crustal-sections through the continental crust: implications for crustal structure, petrology and evolution. *Earth Planet. Sci. Lett.* 56, 263–277.
- Goodwin, A.M., 1991. *Precambrian Geology*. Academic Press, London.
- Gradstein, F.M., Agterberg, F.P., Ogg, J.G., Hardenbol, J., van Veen, P., Thierry, J., Huang, Z., 1994. A mesozoic time scale. *J. Geophys. Res.* 99, 24,051–24,074.
- Haggerty, S.E., 1978. Mineralogical constraints on Curie isotherms in deep crustal magnetic anomalies. *Geophys. Res. Lett.* 5, 105–108.
- Hahn, A., Ahrendt, H., Jeyer, J., Hufen, J.-H., 1984. A model of magnetic sources within the earth's crust compatible with the field measured by the satellite Magsat. *Geol. Jb.* A75, 125–156.
- Harrison, C.G.A., Carle, S.M., Hayling, K.L., 1986. Interpretation of satellite elevation magnetic anomalies. *J. Geophys. Res.* 91, 3633–3650.
- Hayling, K.L., 1991. Magnetic anomalies at satellite altitude over continent-ocean boundaries. *Tectonophysics* 192, 129–143.
- Hemant, K., 2003. Modelling and interpretation of global lithospheric magnetic anomalies. Ph.D. Thesis. Freie Universität, Berlin (<http://www.diss.fu-berlin.de/2003/270/indexe.html>).
- Hemant K., Maus, S., 2004. Geological modeling of the new CHAMP magnetic anomaly maps using a Geographical Information System (GIS) technique. *J. Geophys. Res.*, submitted for publication.
- Hinze, W.J., von Frese, R.R.B., Ravat, D.N., 1991. Mean magnetic contrasts between oceans and continents. *Tectonophysics* 192, 117–127.
- Hunt, C.P., Moskowitz, B.M., Banerjee, S.K., 1995. Magnetic properties of Rocks and Minerals. In: Ahrens, T.J. (Ed.), *Rock Physics and Phase Relations—A Handbook of Physical Constants*. AGU Ref. shelf 3.
- LaBrecque, J.L., Raymond, C.A., 1985. Eafloor spreading anomalies in the Magsat field of the North Atlantic. *J. Geophys. Res.* 90, 2565–2575.
- Langel, R.A., Hinze, W.J., 1998. *The Magnetic Field of the Earth's Lithosphere—The Satellite Perspective*. Cambridge University Press.
- Maus, S., Haak, V., 2003. Magnetic field annihilator: invisible magnetisation at the magnetic equator. *Geophys. J. Int.* 155, 509–513.
- Maus, S., Rother, M., Holme, R., Luehr, H., Olsen, N., Haak, V., 2002. First CHAMP satellite magnetic data resolve uncertainty about strength of the lithospheric magnetic field. *Geophys. Res. Lett.* 29, 14.
- Meyer, J., Hufen, J.-H., Siebert, M., Hahn, A., 1983. Investigations of the internal geomagnetic field by means of a global model of the earth's crust. *J. Geophys.* 52, 71–84.
- Meyer, J., Hufen, J.-H., Siebert, M., Hahn, A., 1985. On the identification of Magsat anomaly charts as crustal part of internal field. *J. Geophys. Res.* 90, 2537–2542.
- Müller, R.D., Roest, W.R., Royer, J.-Y., Gahagan, L.M., Sclater, J.G., 1997. Digital isochrons of the world's ocean floor. *J. Geophys. Res.* 102, 325–338.
- Nataf, H.-C., Ricard, Y., 1996. 3SMAC: an a priori tomographic model of the upper mantle based on geophysical modelling. *Phys. Earth Planet. Int.* 95, 101–122.
- Pohl, J., Pätzold, T., Rolf, C., Soffel, H.C., Worm, H.U., 1991. A rock magnetic log of the KTB pilot borehole. *Sci. Drill.* 2, 120–129.
- Pucher, R., Wonik, T., 1997. Comment on “An interpretation of the Magsat anomalies of central Europe” by Taylor and Ravat. *J. Appl. Geophys.* 36, 213–216.
- Pucher, R., Wonik, T., 1998. A new interpretation of the Magsat anomalies of central Europe. *Phys. Chem. Earth.* 23, 981–985.
- Purucker, M.E., Langel, R.A., Rajaram, M., Raymond, C., 1998. Global magnetization models with a priori information. *J. Geophys. Res.* 103, 2563–2584.
- Purucker, M.E., Dyment, J., 2000. Satellite magnetic anomalies related to sea floor spreading in the South Atlantic ocean. *Geophys. Res. Lett.* 27, 2765–2768.
- Purucker, M.E., Langlais, B., Olsen, N., Hulot, G., Manda, M., 2002. The southern edge of cratonic North America: evidence from new satellite magnetometer observations. *Geophys. Res. Lett.*, 29 (15), ORS 1.
- Raymond, C.A., LaBrecque, J.L., 1987. Magnetization of the oceanic crust: thermoremanent magnetization or chemical remanent magnetization? *J. Geophys. Res.* 92, 8077–8088.
- Royer, J.Y., Müller, R.D., Gahagan, L.M., Lawver, L.A., Mayes, C.L., Nuernberg, D., Sclater, J.G., 1992. A global isochron chart. *Tech. Rep.* 117.38. Institute For Geophysics, University of Texas, Austin.

- Shive, P.N., 1989. Can remanent magnetisation in the deep crust contribute to long wavelength magnetic anomalies? *Geophys. Res. Lett.* 16, 89–92.
- Shive, P.N., Blakely, R.J., Frost, B.R., Fountain, D.M., 1992. Magnetic properties of the lower continental crust. In: Fountain, D.M., Arculus, R., Kay, R.W. (Eds.), *Continental Lower Crust*. Elsevier, Amsterdam, pp. 145–177.
- Singh, B.P., Rajaram, M., Bapat, V.J., 1991. Definition of the continent–ocean boundary of India and the surrounding oceanic regions from Magsat data. *Tectonophysics* 192, 145–151.
- Taylor, P.T., Ravat, D.N., 1995. An interpretation of the Magsat anomalies of central Europe. *J. Appl. Geophys.* 34, 83–91.
- Taylor, P.T., Ravat, D.N., 1997. Reply to comments by R. Pucher and T. Wonik. *J. Appl. Geophys.* 36, 217–219.
- Treloar, N.A., Shive, P.N., Fountain, D.M., 1986. Viscous remanence acquisition in deep crustal rocks. *EOS Trans. Am. Geophys. Union* 67, 266 (Abstract).
- Verhoef, J., Roest, W.R., Macnab, R., Arkani-Hamed, J., et al., 1996. Magnetic anomalies of the Arctic and North Atlantic Oceans and adjacent land areas. Geological Survey of Canada. Open file 3125a (<http://agcwww.bio.ns.ca/pubprod/of3125etc.html>), Canada.
- Wasilewski, P.J., Mayhew, M.A., 1992. The Moho as a magnetic boundary revisited. *Geophys. Res. Lett.* 19, 2259–2262.
- Wahler, K., Purucker, M., 2003. Global models of the lithospheric magnetic field from satellite data. IUGG, Sapporo, Japan.
- White, R.S., McKenzie, D., O’Nions, R.K., 1992. Oceanic crustal thickness from seismic measurements and rare earth element inversions. *Jnl. Geophys. Res.* 97, 19683–19715.
- Worm, H.U., Rolf, C., 1994. Remanent magnetization of KTB drill cores. *Sci. Drill.* 4, 185–196.